Int J Earth Sci (Geol Rundsch) (2011) 100:1433–1450
DOI 10.1007/s00531-010-0592-4

ORIGINAL PAPER

Petrogenetic and geotectonic significance of Neoproterozoic suprasubduction mantle as revealed by the Wizer ophiolite complex, Central Eastern Desert, Egypt

E. S. Farahat · G. Hoinkes · A. Mogessie

Received: 6 March 2010 / Accepted: 6 August 2010 / Published online: 5 September 2010

Abstract Ophiolite complexes, formed in a suprasubduction zone environment during Neoproterozoic time, are widely distributed in the Eastern Desert of Egypt. Their mantle sections provide important information on the origin and tectonic history of ocean basins these complexes represent. The geochemistry and mineralogy of the mantle section of the Wizer ophiolite complex, represented by serpentinites after harzburgite containing minor dunite bodies, are presented. Presence of antigorite together with the incipient alteration of chromite and absence of chlorite suggests that serpentinization occurred in the mantle wedge above a Neoproterozoic subduction zone. Wizer peridotites have a wide range of spinel compositions. Spinel Cr# [100Cr/(Cr + Al)] decrease gradually from dunite bodies (Cr# = 81–87) and their host highly depleted harzburgites (Cr# = 67–79) to the less depleted harzburgites (Cr# = 57–63). Such decreases in mantle refractory character are accompanied by higher Al and Ti contents in bulk compositions. Estimated parental melt compositions point to an equilibration with melts of boninitic composition for the dunite bodies (TiO_2 = ~<0.07–0.22 wt%; Al_2O_3 = 9.4–10.6 wt%), boninitic-arc tholeiite for the highly depleted harzburgites (TiO_2 = <0.09–0.28 wt%; Al_2O_3 = 11.2–14.1 wt%) and more MORB-like affinities for the less depleted harzburgites (TiO_2 = ~<0.38–0.51 wt%; Al_2O_3 = 14.5–15.3 wt%). Estimated equilibrium melts are found in the overlying volcanic sequence, which shows a transitional MORB–island arc geochemical signature with a few boninitic samples. Enrichment of some chromites in TiO_2 and identification of sulfides in highly depleted peridotites imply interaction with an impregnating melt. A two-stage partial melting/melt–rock reaction model is advocated, whereby, melting of a depleted mantle source by reaction with MORB-like melts is followed by a second stage melting by interaction with melts of IAT–boninitic affinities in a suprasubduction zone environment to generate the highly depleted harzburgites and dunite bodies. The shift from MORB to island arc/boninitic affinities within the mantle lithosphere of the Wizer ophiolite sequence suggests generation in a protoarc-forearc environment. This, together with the systematic latitudinal change in composition of ophiolitic lavas in the Central Eastern Desert (CED) of Egypt from IAT–boninitic affinities to more MORB-like signature, implies that the CED could represent a disrupted forearc-arc-backarc system above a southeast-dipping subduction zone.

Keywords Pan-African · ANS · Ophiolites · Serpentinites · Spinels · Egypt

E. S. Farahat (✉)
Department of Geology,
Minia University, El-Minia 61519, Egypt
e-mail: esamfarahat1@yahoo.com

G. Hoinkes · A. Mogessie
Institute of Earth Science (Mineralogy and Petrology),
Karl-Franzens University, Graz, Austria

Introduction

The Eastern Desert of Egypt is part of the Arabian-Nubian Shield (ANS) formed during the Neoproterozoic time. The ANS is good example of Neoproterozoic juvenile crust (Stern and Hedge 1985; Kröner et al. 1992a; Stern 1994; Patchett and Chase 2002). Neoproterozoic basement in the Eastern Desert is characterized by wide distribution of ophiolites, indicating that modern plate-tectonic-like geodynamic processes took place during the ANS evolution.

These ophiolites are the only vestiges of the Precambrian oceanic lithosphere of ocean basins these complexes are thought to represent. Consequently, ophiolites are particularly significant to understand the petrogenetic and geotectonic processes involved in the evolution of the juvenile ANS crust.

The origin and geotectonic evolution of the ophiolites from the Eastern Desert of Egypt has been controversial over the last 30 years. Despite accumulating evidence for their suprasubduction zone origin, debate is currently polarized into whether they are formed by spreading above subduction zone in forearc or backarc basin settings. Most authors (e.g. Amstutz et al. 1984; Khudeir and Asran 1992; El-Sayed et al. 1999; Farahat et al. 2004; El Gaby 2005) adopted backarc basins origin based principally on the transitional MORB–island arc geochemical signature of the volcanic successions that form the ophiolites upper crust. However, the geochemical studies of these ophiolitic volcanic sequences have been challenged by Stern et al. (2004) based on the fact that the geochemical signature of the volcanic rocks could have been affected by crystal fractionation and/or element mobility during alteration and metamorphism. Recently, Stern et al. (2004) and Azer and Stern (2007) argued, based on the chemistry of unaltered chromites found in the mantle sections of these ophiolite complexes, that most—if not all—of them formed in forearc settings. Farahat (2001, 2010) and Farahat et al. (2010) reported a systematic spatial enrichment (from north to south) in the concentration of incompatible trace elements of many ophiolitic metavolcanic rocks occurring in the Egyptian Central Eastern Desert (CED).

Prior to the study of Egyptian ophiolitic peridotites by Azer and Stern (2007), studies of Egyptian ophiolites have focused mainly on the composition of volcanic sequences, for evaluating their tectonic setting. Mantle peridotites of the ophiolite complexes provide, however, important information on the process of melt generation, the relationship with the overlying crustal sections, and the influence of any mantle–melt interaction subsequent to melt extraction (e.g., Dick 1989; Johnson et al. 1990; Hellebrand et al. 2002; Seyler et al. 2007; Choi et al. 2008; Rollinson 2008; Caran et al. 2010). Stern et al. (2004) argued for the significance, and thus the need, of studying the mantle section of these ophiolites, especially their chromite compositions, for better characterization of their origin and evolution. The unaltered mineral chromite has been widely used to identify the former tectonic setting and petrogenetic conditions of the mafic and ultramafic rocks (Dick and Bullen 1984; Arai 1992; Arai and Yurimoto 1994; Barnes and Roeder 2001). This is particularly significant for the altered fragment of the mantle now found in ophiolite sequences (e.g. Zhou and Robinson 1997; Rollinson 2008).

Few studies have dealt with the mantle section of CED ophiolite sequences (e.g. Takla and Noweir 1980; Khudeir et al. 1992; Khudeir 1995; Ahmed et al. 2001; El Bahariya and Arai 2003; Azer and Khalil 2005). These studies focused on small areas that cannot reflect regional variations, nor did the small number of studies reveal compositional differences within each mantle section, which is a significant petrogenetic factor. Azer and Stern (2007) integrated these and other studies to reveal overall variations in CED ophiolitic peridotites. In this work, detailed sampling of serpentinites from the mantle section of the Wizer ophiolite sequence, Central Eastern Desert of Egypt, is carried out. These results are significant as they show important chemical variability of unaltered chromites found in these rocks, from MORB to island arc to boninitic signature. Such chemical variability is genetically related to the overlying volcanic section. These results allow us to investigate the processes, which controlled genesis of the Wizer ophiolite complex and to infer its geotectonic environment. We used this, in conjunction with the published geochemical and mineralogical data from other ophiolite sequences occurring in the CED of Egypt, to propose a new geotectonic evolution model for this part of the Eastern Desert that it could represents a complete forearc-arc-backarc system above a southeast-dipping subduction zone.

General geology

Geological background

Basement rocks in the Eastern Desert of Egypt are part of the ANS which also crop out around the Red Sea in western Arabia, Sinai, Red Sea Hills of Sudan, Eritrea and Ethiopia (Fig. 1). The Neoproterozoic ANS crust was formed by accretion of smaller terranes of arc and backarc crust, generated within and around the margins of the Mozambique ocean (~870–690 Ma, Stern 1994). Some authors have argued, however, for the involvement of pre-Pan-African continental crust or asthenosphere upwelling to account for the high crustal growth rate of the ANS (e.g. Dixon and Golombek 1988; Stein and Hofmann 1994; Farahat 2006; Hargrove et al. 2006). The collision between the complex terranes of East and West Gondwanaland at about 600 Ma (Meert 2003) led to suturing these terranes to the Saharan metacraton. ANS has been cratonized before the development of an extensive peneplain in mid-Cambrian (~520 Ma) and was exhumed in the Tertiary times during Red Sea rifting.

Basement rocks in the Eastern Desert of Egypt are divided into three, lithologically distinguished, domains: North Eastern Desert (NED), Central Eastern Desert (CED)

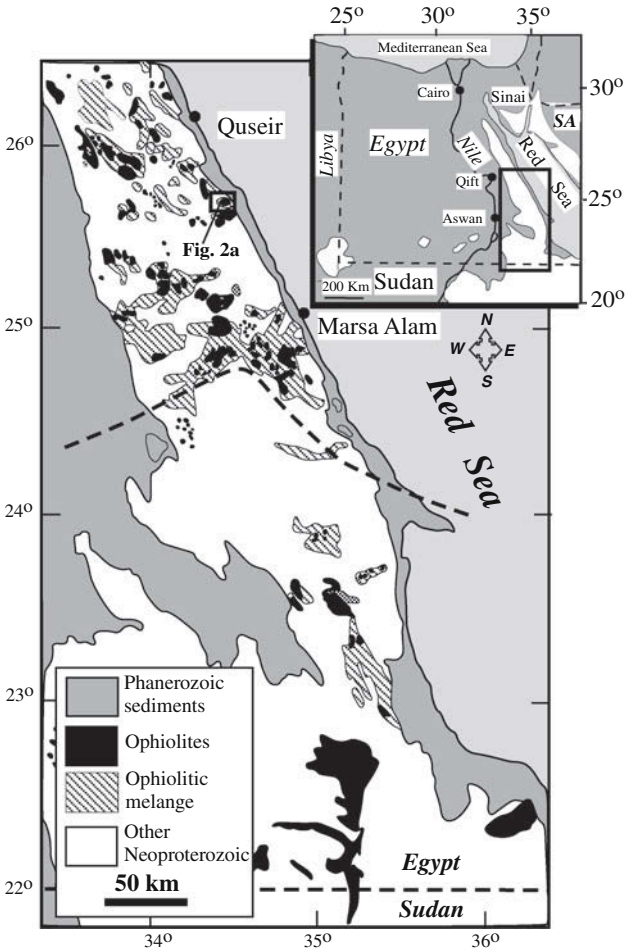

Fig. 1 Map showing the distribution of ophiolites in the central and southern parts of the Eastern Desert of Egypt (modified after Shackleton 1994). The major shear zone (*heavy dashed line*) separating the central and southern parts of the Eastern Desert is from Stern and Hedge (1985). Insert, Neoproterozoic outcrops of the Arabian-Nubian Shield (*white*) in the Eastern Desert of Egypt, Sinai, Saudi Arabia (SA), Sudan and Libya

and Southern Eastern Desert (SED) (Stern and Hedge 1985; El Gaby et al. 1988). The investigated ophiolite complex lies in the CED (Fig. 1), which comprises abundant dismembered ophiolite suites together with island arc meta-volcanosedimentary assemblages, metagabbro-diorite complexes and calc-alkaline granitoids, formed during the arc/backarc stage between ~750 and 620 Ma (Stern 1994). Weakly deformed granodiorites are predominant during the collision stage. Large masses of alkaline granites penetrate this crust during the post-collision, crustal extensional, stage (610–580 Ma) (Abdel Rahman and Doig 1987; Beyth et al. 1994).

Although identified early (Rittmann 1958), the significance of the ophiolites in the Eastern Desert of Egypt was not considered until the recognition of the well-preserved Wadi Ghadir ophiolite sequence by El Sharkawy and El Bayoumi (1979). Since that time, the broadly distributed serpentinites of Egypt were regarded as a member of the commonly dismembered ophiolite suites that are tectonically obducted in convergent zones (e.g. El Gaby et al. 1988; Kröner et al. 1992b; Abu El Ela 1996). However, some authors (e.g. Akaad 1997; Akaad and Abu El Ela 2002; Ahmed 2005) raised doubt on the ophiolitic affinity of some serpentinites and considered them as representing intruded magmas. Yet, Azer and Stern (2007) re-emphasized the ophiolitic nature of the Egyptian serpentinites and related the intrusive appearance of some of these rocks to their different structural position in surrounding rocks, along with their much weaker and easier deformation behavior compared to their country rocks.

The investigated Wizer ophiolite sequence and associated volcano-sedimentary association have been studied earlier by some authors (e.g. Hume 1935; Sabet 1961; Noweir et al. 1983) in the light of the geosynclinal concept. More recently, Khudeir and Asran (1992) suggested a backarc basin origin for this ophiolite sequence based on the geochemical characteristics of its volcanic section.

Field relations and petrography

The investigated Wizer area is occupied mainly by an ophiolite suite that is composed mainly of an ophiolite mélange and a remnant ophiolite nappe (Fig. 2a). The ophiolite sequence is folded into a major NW-trending syncline (Khudeir and Asran 1992). The ophiolite nappe occupies the trough of the syncline and tectonically overlies the ophiolitic mélange.

According to Akaad and Abu El Ela (2002), the mélange matrix in the area consists chiefly of regionally metamorphosed layered volcaniclastic turbidites (metaconglomerates, metagreywackes, metamudstones and schists) enclosing fragments of ophiolitic serpentinites, metagabbros and metavolcanics.

The remnant ophiolite nappe comprises serpentinites, metagabbros and metabasalts (Khudeir and Asran 1992). Serpentinites are the major unit preserved in the Wizer ophiolite. They form N- to NW-trending thrust sheets overlying the ophiolitic mélange, NW-trending narrow belts between metavolcanics and metagabbros, and as small fragments embedded in the mélange matrix. Serpentinites are homogenous or poorly schistose and consist largely of entirely serpentinized peridotites. In addition, minor brownish to brownish black dunite forms rounded to lensoidal bodies and small bands parallel to the tectonic fabric of peridotites are occasionally recognized at the deep parts of the serpentinite sheets, from ~10 to 40 cm in size (Fig. 3a). In places, dunite bodies are heterogeneous in composition, deformed and containing numerous carbonate veinlets. Adjacent to faults and fractures, where alteration

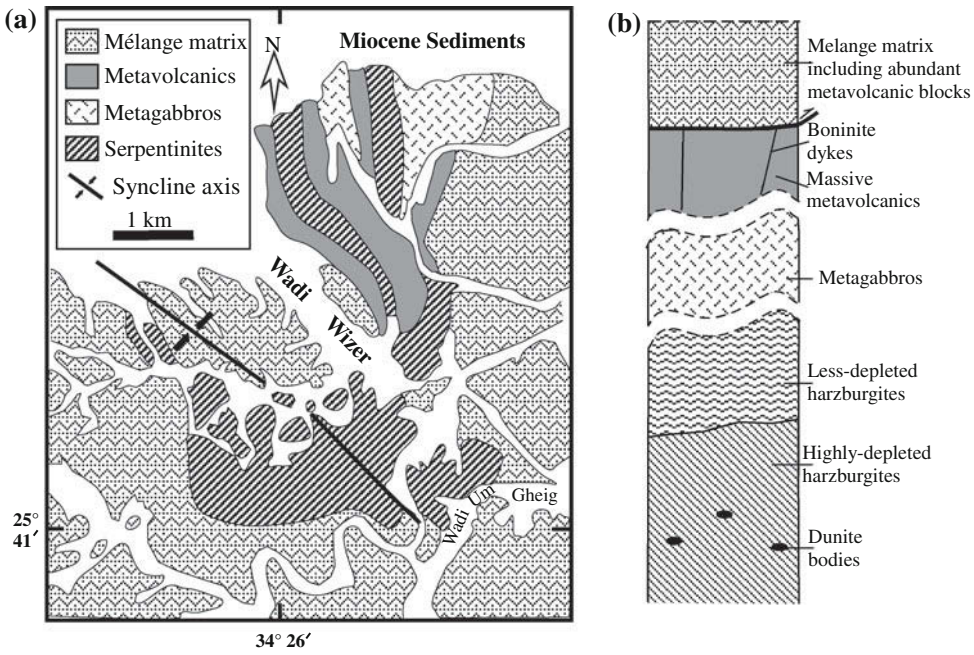

Fig. 2 **a** Geological map of the Wizer ophiolite sequence (Modified after Khudeir and Asran 1992; Akaad and Abu El Ela 2002). **b** Synthetic pseudo-stratigraphies (not to scale) of the Wizer ophiolite

is most intense, serpentinites are highly sheared and altered to ta lc-carbonates. As we aim to investigate the petrogenetic evolution of the mantle section of this ophiolite sequence, sampling of these highly altered serpentinites was avoided. Having this in mind, the best preserved and most homogenous thrust sheets were systematically sampled from bottom to top, although details of peridotite structure are not clear because of the extensive deformation. Also, the contact between the mantle and crust is seldom exposed, and the original Moho is nowhere preserved. Synthetic pseudo-stratigraphies of the Wizer ophiolite, dismembered but nearly intact sequence, are presented in Fig. 2b.

Metabasalts and metagabbros occur as fault-controlled blocks that typically form small elongated patches (up to 5 km long) within the serpentinites in the trough of the syncline. The ophiolitic metavolcanics and metagabbros are tectonically juxtaposed against the serpentinized mantle section. Consequently, the original internal architecture of the Wizer ophiolite was tectonically disrupted during its emplacement.

Petrographical and X-ray diffraction (XRD) studies have revealed that the investigated peridotites are entirely serpentinized harzburgites and subordinate dunites composed of antigorite with accessory carbonates, magnetite, chromite and sulfides. The harzburgitic composition of the Wizer serpentinized peridotite is indicated by the abundance of bastite texture (Fig. 3b) with magnetite striations along the cleavage plane of the original orthopyroxene crystals. By contrast, such bastite texture is completely lacking in dunites. The latter are composed of serpentine that show the original form, and *Y*-shape cracks, of olivine. Carbonates are represented mainly by dolomite and less abundant magnesite as disseminated fine aggregates and veinlets. Serpentinized dunite bodies are small, heterogeneous in composition and contain more carbonate veinlets. Accessory sulfides are rarely dispersed throughout the harzburgites but absent from dunites.

Chromites in harzburgites (up to 7%) are represented by euhedral to subhedral crystals incipiently altered along rims to Cr-magnetite (Fig. 3c, d). However, dunites contain chromites, which vary from subhedral to anhedral grains with lobate boundaries, also incipiently altered along margins and fractures to Cr-magnetites (Fig. 3e). The modal volume of spinel from the dunite bodies is generally similar to that of the host harzburgites, but a few thin bands of disseminated chromitite are occasionally present. A transitional zone of ferritchromite between the unaltered core and Cr-magnetite outer margin is seldom recorded (Fig. 3f).

Methods

All analyses were made at the Institute of Earth Sciences (Mineralogy and Petrology), Karl Franzens University, Graz, Austria. Mineral analyses and backscattered electron images were done on a JEOL-JSM 6310 scanning electron microscope with Oxford ISIS EDX and Microspec WDX (15 kv, 6 nA, Na with TAP, all other elements on EDX) and on a JEOL JXA-8200 electron microprobe at the Eugen F. Stumpfl microprobe lab at Leoben (15 kv, 10 nA,

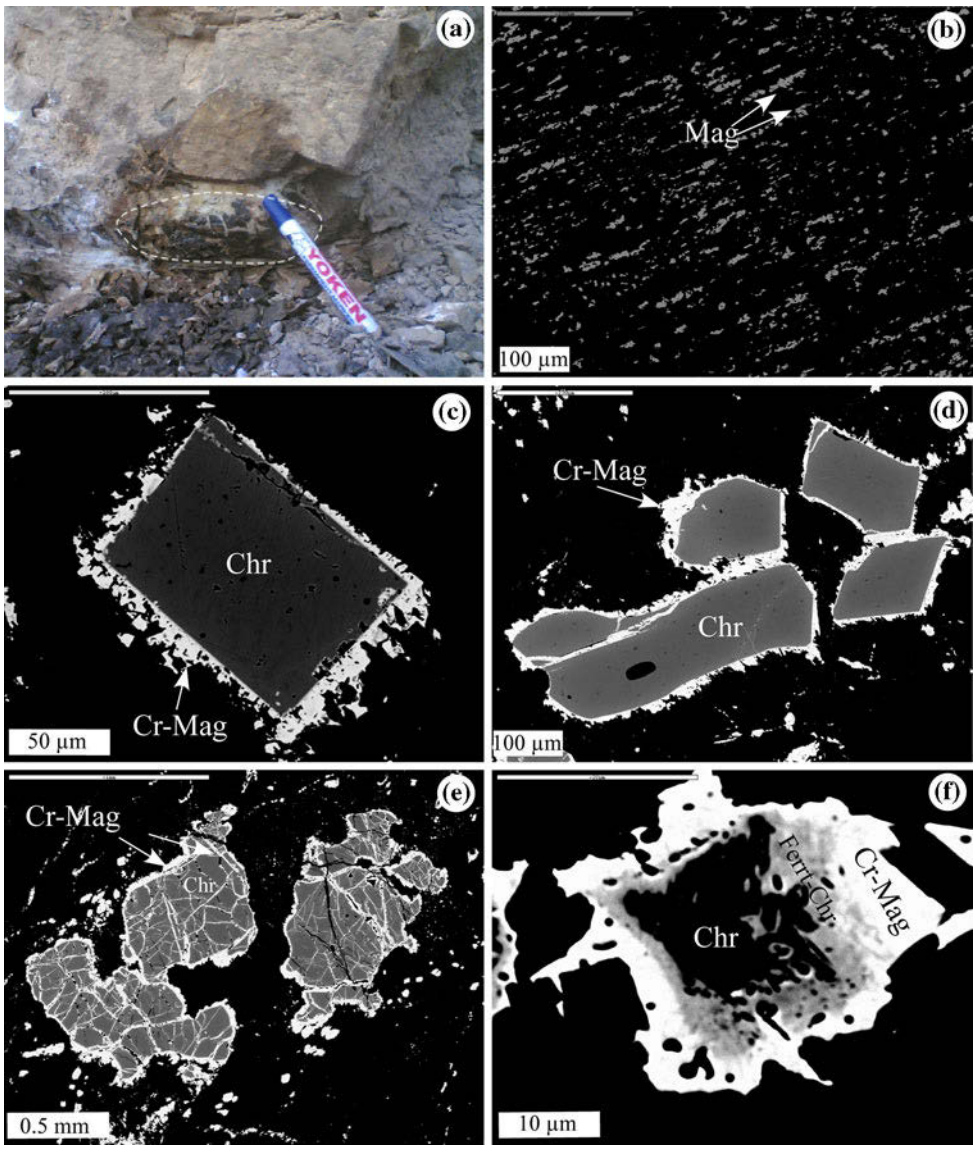

Fig. 3 **a** Photograph showing the lower mantle section of serpentinites with dunite lens. Images **b–f** are back-scattered electron images (*BSE*). **b** Bastite texture composed of magnetites (*Mag*) that define cleavage planes of original orthopyroxene crystal. **c** Euhedral crystal and **d** Euhedral to subhedral crystals of chromites (*Chr*) in harzburgites incipiently altered to Cr-magnetite (*Cr-Mag*) along rims. **e** Chromite crystals in dunite with lobate boundaries and incipiently altered to Cr-magnetite along fractures and rims. **f** Primary chromite (*Chr*) altered to ferritchromite (*Ferrit-Chr*) and Cr-magnetite outer rims (*Cr-Mag*)

5 WDX-spectrometers). A range of natural and synthetic minerals was used as standards. The analyses were normally done at a magnification of spot mode. The matrix correction was calculated with ZAF-correction program. Fe^{2+}–Fe^{3+} redistribution from electron microprobe analyses is made using the charge balance equation of Droop (1987) for estimating Fe^{3+}.

Whole-rock major and trace element contents of peridotites were obtained with a Bruker Pioneer S4 X-ray fluorescence (XRF) spectrometer. Fused glass discs using $Li_2B_4O_7$ flux were used for major oxides, whereas pressed powder pellets were used for trace element determinations. Loss on ignition (LOI) was determined by heating powdered samples for 1 h at 1,000°C. The analytical precision and accuracy is better than 3% of the amount present for major elements and 10% for trace elements. Selected samples of serpentinized peridotites and dunites were subjected to X-ray diffraction (XRD) analyses to determine their mineralogical compositions using Siemens D5000 diffractometer.

Geochemistry

Bulk-rock chemistry

Whole-rock chemical analyses of the investigated serpentinites are given in Table 1. All whole-rock major and trace element data are reported on a volatile-free basis to estimate the near-protolith compositions. Generally, the Wizer serpentinites show limited variations in their compositions. They are characterized by high contents of SiO_2 (42.09–46.63 wt%) and MgO (42.72–47.61 wt%) and high Mg# (molar 100 Mg/Mg + Fe^{2+}, 89–93). However, Al_2O_3

Table 1 Major oxides and trace element data of serpentinites from Wizer ophiolite

	Less depleted harzburgites			Highly depleted harzburgites				Dunite bodies		
SiO_2 (wt%)[a]	44.93	45.90	45.41	43.90	45.23	42.66	46.63	43.52	42.09	43.41
TiO_2	0.04	0.04	0.02	0.02	0.02	0.03	0.03	0.00	0.02	0.02
Al_2O_3	1.04	0.68	0.81	0.50	0.62	0.59	1.00	0.30	0.51	0.42
Fe_2O_3	8.55	9.61	8.49	8.74	8.94	0.33	8.31	9.13	8.99	7.31
MnO	0.12	0.15	0.10	0.14	0.15	0.17	0.12	0.18	0.16	0.11
MgO	44.53	42.72	44.24	45.38	44.56	46.71	43.64	45.96	47.15	47.61
CaO	0.52	0.70	0.81	1.16	0.41	0.46	0.12	0.85	1.05	0.97
Na_2O	0.17	0.09	0.08	0.12	0.00	0.00	0.08	0.04	0.00	0.10
K_2O	0.01	0.04	0.01	0.00	0.01	0.00	0.00	0.00	0.00	0.00
TiO_2	0.04	0.04	0.02	0.02	0.02	0.03	0.03	0.00	0.02	0.02
P_2O_5	0.03	0.04	0.01	0.03	0.04	0.02	0.02	0.04	0.02	0.02
Sum	100.00	100.00	100.00	100.00	100.00	100.00	100.00	100.00	100.00	100.00
LOI[b]	14.46	14.82	13.13	16.74	13.8	15.97	11.89	15.64	15.54	15.54
Mg#	91	90	91	91	89	91	91	91	91	93
CIPW norm[c]										
Ol	66	59	63	75	38	70	57	77	82	80
Opx	28	34	29	18	56	16	39	11	10	14
Cpx	4	4	4	5	5	2	0	7	4	5
Trace elements										
Ba (ppm)	6.4	53.7	16.1	14.4	79.5	27.4	48.5	41.3	36.3	33.2
Co	103	127	112	132	124	126	107	115	105	115
Cr	2,559	2,723	2,737	3,009	3,071	3,539	2,889	4,691	4,692	4,419
Cs	<2	6.9	<2	<2	6.0	6.5	14.0	<2	29.0	<2
Cu	20.1	24.6	26.5	6.6	49.8	10.3	40.1	6.8	11.7	10.5
Ga	2.2	<2	<2	4.6	0.7	6.8	2.2	<2	<2	<2
Mo	<2	4.2	<2	<2	7.1	<2	<2	5.4	<2	2.1
Nb	<2	<2	<2	<2	<2	<2	<2	<2	<2	<2
Ni	2,357	2,925	2,455	2,657	3,054	2,559	2,485	3,361	3,839	3,256
Pb	8.0	<2	5.6	9.2	<2	6.1	<2	<2	<2	<2
Rb	1.6	0.6	0.0	2.8	0.9	1.4	0.0	0.2	1.9	0.0
Sc	8.4	5.0	10.1	<2	6.7	<2	<2	5.2	7.9	5.7
Sr	43	45	33	59	19	33	23	127	113	120
U	<2	2.9	<2	7.7	<2	<2	5.7	<2	5.6	<2
V	41	52	44	38	48	36	44	38	36	32
Y	3	<2	<2	<2	<2	<2	1.1	<2	<2	<2
Zn	49	48	48	163	74	70	69	96	93	67
Zr	8.2	4.1	6.1	<2	<2	18.5	13.6	4.6	2.3	3.0

[a] Major elements (wt%) recalculated to 100% anhydrous compositions

[b] LOI = loss on ignition values before normalization to volatile-free compositions

[c] calculated CIPW norm following the scheme by Niu (1997)

and CaO contents are low and variable (0.30–1.04 and 0.12–1.16 wt%, respectively). Na_2O (<0.17 wt%) and TiO_2 (<0.04 wt%) are very low. Extensive serpentinization of the investigated rocks is indicated by their high water contents (loss on ignition LOI values), ranging from 11.89 to 16.74 wt%.

CIPW norm calculations, following the calculation scheme of Niu (1997), classify the Wizer serpentinites as harzburgites in agreement with the petrographic examination, except for dunite bodies. The latter are small, containing many carbonate veinlets and heterogeneous in hand specimen, thus their composition is most likely

influenced by the CO_2-metasomatism and variation in modal amounts of coarse-grained chromites and/or chromitite-like veins. Nevertheless, they display higher normative olivine contents (76.52–81.89%) compared to harzburgites (59.14–74.51%). However, the high clinopyroxene normative contents in dunites may be related to addition of Ca due to CO_2-metasomatism.

Regarding trace element compositions, Cr and Ni contents are generally high. Dunites are richer in these two elements (4,419–4,692 ppm and 3,256–3,839 ppm, respectively) relative to harzburgites (2,559–3,539 ppm and 2,357–3,054 ppm, respectively). Cobalt shows little variation (103–132 ppm). Zn and V contents vary from 48 to 163 ppm and 32 to 52 ppm, respectively. However, the contents of Ba, Cs, Cu, Pb, U and Sr are highly variable, implying possible redistribution associated with serpentinization. Concentrations of all other trace elements are very low.

In general, major elements (except Na, K and P) and trace elements, except Pb and U, are considered conservative during serpentinization (e.g. Niu 2004; Paulick et al. 2006). The high and restricted ranges of Mg#, Cr and Ni, together with the very low contents of Ca, Al, Ti and incompatible trace elements, indicate that most major elements (SiO_2, MgO, Al_2O_3, CaO, TiO_2) and trace elements (at least Cr, Ni, Co, Zn) can be used to infer the melting conditions and tectonic setting of the protoliths. The low Al_2O_3 and CaO contents of the investigated peridotites are closely analogous to that observed for forearc peridotites and different from those of the MOR peridotites (Fig. 4). On the other hand, the high Mg# of Wizer serpentinites along with their enrichment in Cr, Ni and Co and depletion in other incompatible trace elements suggest significant melt depletion of the protoliths. Moreover, the general progressive decrease in Al_2O_3 and TiO_2 contents from harzburgites to dunites reflects progression from less-refractory to ultra-refractory character as will be discussed later in detail.

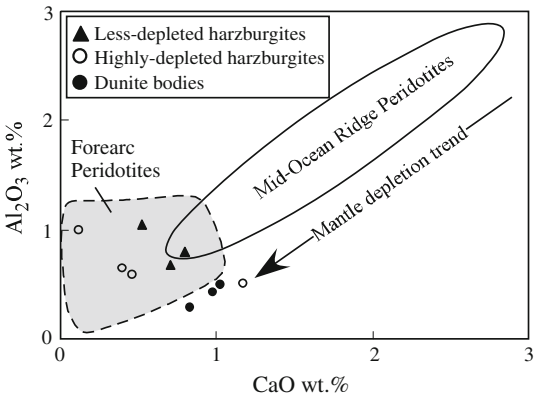

Fig. 4 Whole-rock CaO versus Al_2O_3 variation diagram for the Wizer serpentinites. Fields of forearc and mid-ocean ridge peridotites are from Ishii et al. (1992)

Mineral chemistry

Chromites

Representative compositions of chromite from the Wizer serpentinites are given in Table 2. The range of chromite compositions from both cores and rims on one hand and from cores on the other hand is broad. Such variability in chromite composition is distinctively characterized on Al–Cr–Fe^{3+} triangular plot (Fig. 5). Compared to cores, the rarely recorded ferritchromite zones are extensively depleted in Al (0.24–4.56 vs. 5.88–22.76 wt% Al_2O_3) but preserve most of their Cr content (29.75–43.23 vs. 44.44–63.74 wt% Cr_2O_3) and consequently lie midway along the Cr–Fe join. However, the outer rims are Cr-magnetite highly depleted in Al but variably depleted in Cr (<0.78 wt% Al_2O_3 and 0.15–22.67 wt% Cr_2O_3).

The chromite cores vary also widely among the investigated samples and help to identify three distinct groups of mantle peridotites in the Wizer ophiolite. The dunites contain Cr-rich (59.15–63.74 wt% Cr_2O_3), Al-poor chromites that cluster close to the Cr-apex, having little variability in Al contents (5.88–9.16 wt% Al_2O_3). Compared to dunite bodies, chromites from the host harzburgites are less enriched in Cr (51.43–60.44 wt% Cr_2O_3) and more enriched in Al (10.66–19.04 wt% Al_2O_3). However, other harzburgites have chromites with the lowest Cr concentration (44.44–49.47 wt% Cr_2O_3) and the highest Al (19.08–22.76 wt% Al_2O_3) concentration. Generally, Cr-rich (i.e. highly depleted) spinels dominate over the less depleted ones.

The considerable diversity among the investigated serpentinites can best be illustrated with the plot of Cr# [molar100Cr/(Cr + Al)] versus Mg# [molar 100 Mg/(Mg + Fe^{2+})] in chromite cores (Fig. 6). The dunite bodies contain chromite cores with high and narrow range of Cr# (81.52–87.64) and relatively wide range of Mg# (36.36–64.17). They plot in/or close to the boninite field and almost follow the trend of fractional crystallization of olivine: spinel (99:1) assemblage from a boninite parent (Bédard and Hébert 1998). On the other hand, the host harzburgites contain chromites that plot over a relatively broad range of Cr# (67.04–79.18), showing a linear covariation with Mg# (38.16–66.77), i.e. partial melting trend and resemble spinels from forearcs (Fig. 6a, b). However, chromites in the less depleted harzburgites have relatively low Cr# (57.22–63.48) and high Mg# (50.61–66.27), which also plot in the forearc fields but close to, or within, the depleted end of the abyssal peridotite and MORB array in both diagrams, implying more

Table 2 Representative compositions (wt%) of chromites from the mantle of the Wizer ophiolite sequence

	Less depleted harzburgites									
	L-8c*	L-8fr	L-8r	L-9c	L-9fr	L-9r	L-11c	L-11r	L-4c	L-4r
SiO_2	0.36	0.35	0.27	0.21	0.30	0.39	0.27	0.30	0.25	0.30
TiO_2	0.06	0.15	0.00	0.03	0.07	0.00	0.00	0.00	0.03	0.03
Al_2O_3	21.42	0.34	0.39	20.21	0.70	0.48	20.80	0.26	22.75	0.27
Cr_2O_3	45.68	30.85	0.84	46.19	36.18	3.20	47.72	19.82	45.58	4.60
Fe_2O_3	2.27	36.86	67.45	3.04	30.82	64.55	2.67	47.92	1.07	62.93
FeO	16.92	25.83	29.51	18.40	24.77	29.30	13.07	26.17	17.39	28.64
MnO	0.46	3.44	0.10	0.17	3.71	0.47	0.28	2.13	0.18	0.20
MgO	11.89	1.09	0.40	10.58	1.51	0.51	14.38	0.96	11.78	0.65
CaO	0.00	0.00	0.07	0.15	0.00	0.00	0.06	0.10	0.02	0.02
ZnO	0.12	0.59	0.00	0.43	0.65	0.00	0.00	0.47	0.02	0.09
NiO	0.00	0.77	1.30	0.00	0.54	1.19	0.00	1.30	0.10	1.40
Total	99.18	100.27	100.33	99.40	99.25	100.09	99.25	99.43	99.17	99.12
Cr#	58.88	98.38	58.14	60.53	97.19	81.36	60.61	98.02	57.35	92.11
Mg#	55.61	7.02	2.383	50.61	9.756	3.011	66.27	6.102	54.7	3.858
	Less depleted harzburgites					Highly depleted harzburgites				
	L-6c	L-6r	L-7c	L-7r	L10-c	H-1c	H-3c	H-3r	H-1c	H-1r
SiO_2	0.26	0.34	0.00	0.22	0.23	0.37	0.24	0.65	0.22	0.41
TiO_2	0.01	0.04	0.01	0.05	0.14	0.02	0.10	0.05	0.10	0.00
Al_2O_3	21.03	0.19	21.44	0.33	19.54	14.80	16.21	0.23	10.73	0.41
Cr_2O_3	48.16	0.50	47.61	4.06	48.66	52.86	52.85	3.46	60.05	0.49
Fe_2O_3	1.25	68.34	1.84	64.66	1.12	2.98	2.50	63.59	0.88	67.06
FeO	16.32	28.41	15.94	28.62	16.80	15.63	15.84	30.35	16.13	27.77
MnO	0.44	0.32	0.10	0.29	0.34	0.42	0.16	0.04	0.32	0.14
MgO	12.01	1.00	12.47	1.54	11.58	11.97	12.46	0.57	11.46	1.38
CaO	0.14	0.23	0.09	0.09	0.04	0.03	0.06	0.04	0.11	0.01
ZnO	0.47	0.00	0.00	0.10	0.23	0.28	0.00	0.05	0.03	0.02
NiO	0.02	1.24	0.08	0.00	0.04	0.00	0.00	0.57	0.00	1.32
Total	100.11	100.60	99.57	99.96	98.72	99.36	100.42	99.60	100.04	99.01
Cr#	60.56	65.22	59.84	89.05	62.55	70.57	68.61	91.3	78.97	44.12
Mg#	56.78	5.858	58.21	8.753	55.13	57.7	58.37	3.284	55.87	8.144
	Highly depleted harzburgites									
	H-13c	H-13fr	H-13r	H-7c	H-7r	H-2c	H-2r	H-6c	H-11c	H-111r
SiO_2	0.34	0.21	0.26	0.33	0.36	0.36	0.32	0.35	0.37	0.25
TiO_2	0.06	0.00	0.00	0.00	0.13	0.00	0.02	0.05	0.15	0.01
Al_2O_3	10.66	9.43	0.11	11.44	0.13	13.45	0.10	16.58	14.02	0.04
Cr_2O_3	60.44	59.30	0.59	56.40	6.21	56.42	6.36	53.26	56.09	1.19
Fe_2O_3	0.63	1.20	67.10	0.85	61.01	0.77	61.67	1.66	1.64	69.10
FeO	17.42	19.70	28.52	19.85	28.05	18.42	24.33	14.77	13.88	26.26
MnO	0.54	1.25	0.01	1.43	0.32	0.41	0.38	0.30	0.27	0.20
MgO	10.79	8.02	0.36	7.51	0.41	10.27	2.58	12.92	13.38	2.49
CaO	0.07	0.03	0.03	0.03	0.02	0.02	0.00	0.05	0.08	0.04
ZnO	0.00	0.48	0.00	1.33	0.18	0.22	0.22	0.39	0.20	0.00
NiO	0.00	0.00	2.03	0.00	2.37	0.00	2.20	0.03	0.01	1.40
Total	100.95	99.62	99.01	99.17	99.19	100.34	98.19	100.36	100.08	100.97
Cr#	79.18	80.83	78.26	76.79	96.92	73.8	97.47	68.3	72.85	94.59
Mg#	52.46	42.07	2.222	40.28	2.586	49.85	15.87	60.93	63.2	14.48

Table 2 continued

	Dunite bodies									
	D-4c	D-4r	D-8c	D-8r	D-2c	D-2r	D-14c	D-14r	D-9c	D19-c
SiO_2	0.12	0.16	0.13	0.22	0.25	0.25	0.22	0.36	0.23	0.36
TiO_2	0.15	0.01	0.00	0.00	0.03	0.00	0.04	0.02	0.01	0.01
Al_2O_3	7.82	0.19	7.44	0.18	7.97	0.04	8.22	0.12	7.68	8.68
Cr_2O_3	61.12	0.32	61.39	5.82	61.87	4.24	63.41	3.91	60.29	62.12
Fe_2O_3	1.91	67.48	2.63	62.97	1.15	65.35	0.87	64.61	1.73	0.00
FeO	17.45	26.63	19.25	26.20	19.30	25.06	16.15	25.18	18.89	19.33
MnO	0.47	0.16	0.76	0.23	0.57	0.20	0.16	0.19	1.07	0.15
MgO	10.00	1.30	8.59	1.94	9.00	2.48	11.35	2.55	8.08	9.00
CaO	0.05	0.06	0.06	0.00	0.00	0.00	0.07	0.00	0.10	0.06
ZnO	0.00	0.00	0.32	0.10	0.13	0.19	0.14	0.01	0.85	0.00
NiO	0.00	1.93	0.07	1.83	0.00	2.27	0.00	2.05	0.00	0.00
Total	99.09	98.24	100.63	99.49	100.27	100.09	100.64	99.00	98.93	99.71
Cr#	83.99	52.63	84.68	95.63	83.87	98.44	83.79	95.93	84.06	82.78
Mg#	50.55	7.996	44.28	11.68	45.4	14.96	55.61	15.33	43.28	45.35

Mg# = molar 100 Mg/(Mg + Fe^{2+}), Cr# = molar 100 Cr/(Cr + Al), *c, fr, and r = core, ferritchromite zone and Cr-magnetite rim, respectively

MORB affinity. These chromites almost follow the olivine fractionation trend of Dick and Bullen (1984). It is worth to mention that chromite compositions from the mantle section of the Wizer ophiolite complex almost cover the entire range of compositional variations of chromites from serpentinites in the CED.

TiO_2 contents of Wizer chromites are generally low (<0.17 wt%) but highly variable even within the same sample and/or grain. Such very low TiO_2 content is characteristic of chromites from suprasubduction zone environments. The highest Ni content is recorded from the outer Cr-magnetites especially those of the dunite bodies (up to 2.77 wt%). By contrast, the Mn and Zn are partitioned mainly into the ferritchromite zone compared to both outer magnetite rims and cores.

To better understand the element distribution within zoned chromite grains due to alteration, an electron microprobe analyses profile across one of these grains is presented (Fig. 7). This compositional profile shows that the outer ferritchromite zone and Cr-magnetite rims are significantly depleted in Al and Mg. However, Cr is slightly depleted in ferritchromite compared to the core, but highly depleted in Cr-magnetite outer rim. By contrast, both Fe and Ni are highly enriched at the rim. Mn and Zn are the only elements that do not display systematic variations from core to rim. These two elements are concentrated in the ferritchromite zone compared to unaltered core and the outer Cr-magnetite rim. On the other hand, TiO_2 content is generally very low but with an erratic pattern from core to rim.

Serpentine

The serpentine minerals show almost homogenous chemical composition with no significant variations between those of serpentinized dunites and harzburgites, implying one serpentine generation. Table 3 shows representative chemical analyses of the Wizer serpentine minerals. They contain 43.35–47.20 wt% SiO_2, 37.9–42.15 wt% MgO, 0.07–0.55 wt% Al_2O_3, 0.93–3.67 wt% FeO and 0.02–0.61 wt% Cr_2O_3. The low Al_2O_3 contents and high Si/Mg ratio of the Wizer serpentine support their antigorite composition as revealed by petrographical and XRD studies.

Carbonates

Carbonate alteration of ultramafic rocks has been related to interaction with cold sea water at hydrothermal vents (Palandri and Reed 2004) or with CO_2-rich fluids released from sediments during regional metamorphism or upward from the mantle (Stern and Gwinn 1990). Carbonates in Wizer serpentinites, both as disseminated and in veinlets, are represented mainly by dolomite (11.48–21.14 wt% MgO, 28.71–36.06 wt% CaO; 0.03–2.23 wt% FeO) with less abundant magnesite (46.95–48.17 wt% MgO, 1.04–2.13 wt% FeO).

Sulfides

Rare sulfides are represented by NiS with traces of NiAsS along margins.

Discussion

Alteration effect

Because the Wizer mantle section is entirely serpentinized and the Egyptian basement rocks have been regionally

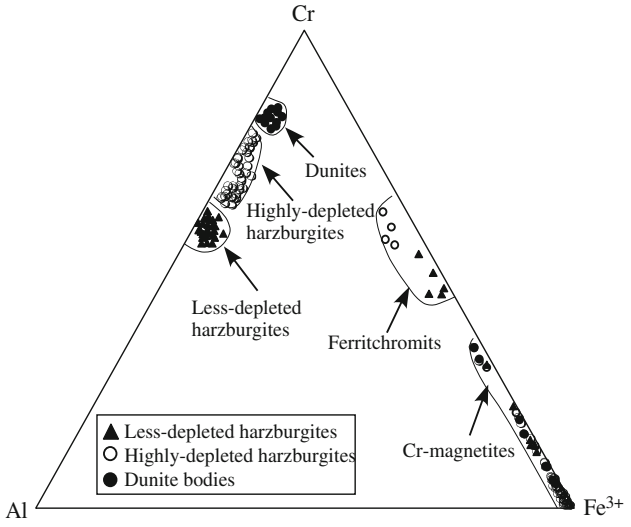

Fig. 5 Ternary plot of the trivalent Al, Cr, Fe^{3+} cations of the chromites from the Wizer serpentinites

metamorphosed up to transitional greenschist–amphibolite facies (e.g. Farahat 2008), any resulting changes in their chromite compositions need to be evaluated before we can use these compositions to make inference about the petrogenetic and geotectonic evolution of the host serpentinites.

The narrow compositional variations of the Wizer serpentine minerals point most likely to one stage of serpentinization. The fact that the serpentine minerals are mainly antigorite, together with the incipient alteration of chromites and absence of chlorite, signifies that these peridotites have been serpentinized in the mantle wedge above a subduction zone and escaped latter regional metamorphism during and after obduction. Antigorite is in general the stable serpentine mineral in ultramafic rocks metamorphosed under the moderate temperatures of blueschist and greenschist facies conditions and is stable to 620°C at 1 GPa (Evans 1977; Ulmer and Trommsdorf 1995). Hyndman and Peacock (2003) documented wide range of geophysical and geological evidences for the extensive serpentinization in the forearc mantle. Large volumes of aqueous fluids released from subducting plates cool the overlying forearc such that the antigorite is stable in the forearc mantle. This could imply the formation of Wizer ophiolites in forearc setting, supporting inference from chromite compositions. In contrast, smaller volumes of fluids are expected to be released beneath the arc and backarc mantles that are commonly less serpentinized.

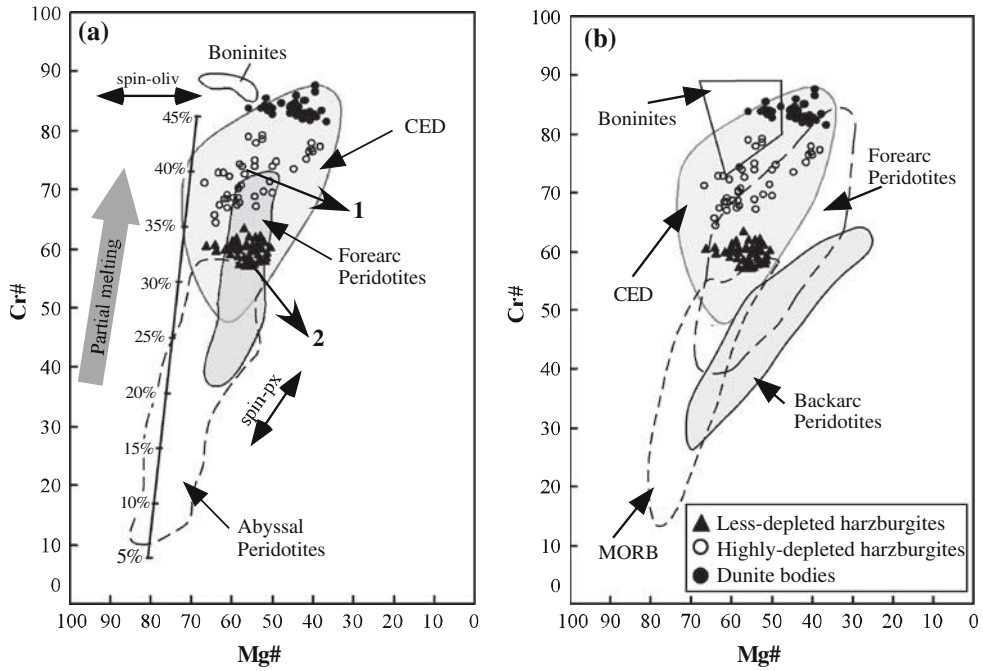

Fig. 6 Spinel core compositions from the Wizer serpentinites, in terms of Cr# versus Mg#. Data for different tectonic environments were compiled from the literature by Pagé et al. (2008) for (**a**) and by Stern et al. (2004) for (**b**). Field for chromite compositions occurring in serpentinites from the Central Eastern Desert of Egypt (*CED*) is also shown (Khudeir 1995; Ahmed et al. 2001; Azer and Khalil 2005; Khalil and Azer 2007; Farahat 2008). Experimental equilibrium-melting trend annotated by melting % is from Hirose and Kawamoto (1995). *Double arrows* labeled spin-oliv and spin-px show the expected trends of variations from spinel and olivine, and spinel and pyroxene subsolidus re-equilibration, respectively (Bédard and Hébert 1998). *Arrow 1* shows olivine: spinel (99:1) fractional crystallization (8–25%) trend from boninite (Bédard and Hébert 1998). *Arrow 2* shows olivine fractionation trend (Dick and Bullen 1984)

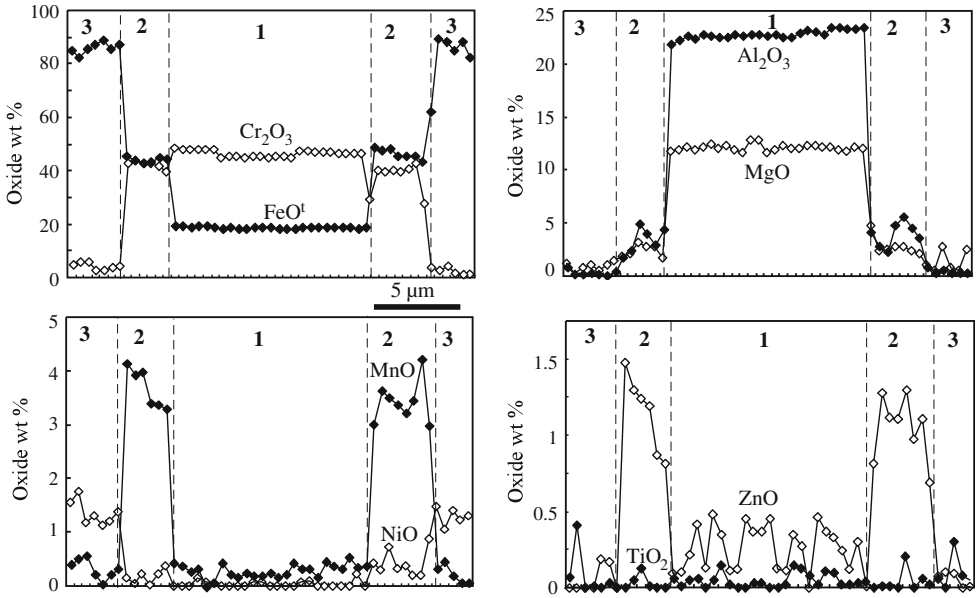

Fig. 7 Chemical profiles of major and minor elements across a spinel (Fig. 2f), which shows a transitional zone of ferritchromite (*2*) between the unaltered core (*1*) and Cr-magnetite rim (*3*)

Stern and Gwinn (1990) ascribed the frequent association of carbonates with the ANS ophiolitic serpentinites to interaction with CO_2-rich fluids released from the mantle rather than from the sediments during regional metamorphism. The abundance of carbonate veinlets within the investigated peridotites and particularly in dunite bodies supports their mantle origin and compatible with their serpentinization in the mantle wedge.

Generally, the investigated spinels are commonly altered to thin film of Cr-magnetite along margins or fractures. Transitional zone of ferritchromite between the magnetite rim and the unaltered core is seldom recorded. To assess the effect of magmatic circulations and/or subsolidus re-equilibration on the chromite core compositions, at least four rimward analyses have been carried out on cores of many chromite grains. Core-rim spinel compositional variations diagram (Fig. 8) shows that, except for slight rimward enrichments in Fe (trend 2, Fig. 8) and in Fe and Cr (trend 3, Fig. 8), the spinel cores are generally unzoned. The rimward Fe enrichment is believed to be related to Fe–Mg exchange with olivine during the slow cooling in the mantle. However, the slight rimward Fe- and Cr enrichment especially in chromites of dunites is attributed to partial melting. Consequently, the chromite cores can be reliably used for determination of the melt evolution and tectonic setting of the host peridotites. Yet varying core compositions in different grains of the same samples are considered to reflect magmatic evolution (e.g. Rollinson 2008).

The compositional profile across zoned chromite grain (Fig. 7) shows that Fe, Ni, Mn and Zn are introduced into chromite composition along the rim most likely from olivine during serpentinization. However, Al, Mg and Cr are all diffused out of the chromites onto antigorite during this process. The spiked patterns of Ti are most likely related to mixing process during magma evolution, as will be discussed latter. It seems that ferritchromite is the favorable receptor of Mn and Zn released from primary minerals during serpentinization (e.g. Farahat 2008). However, the outer Cr-magnetite rims received most of the Ni released from olivine. The highest concentrations of Ni are recorded from the Cr-magnetite rims of chromites in dunite bodies, which further support their dunitic compositions. The slight diffusion of Al, Mg and Cr out of chromite grains during serpentinization could account to their incipient alteration and absence of Cr-chlorite (kammererite) from these rocks. Chlorites formation requires release of large amounts of Al and Mg out of chromites. This is usually attained during regional metamorphism after serpentinization (Barnes 2000; Farahat 2008), which is clearly not the case of the investigated serpentinites.

Parental melt composition and relation to the overlying volcanic sequence

As early mentioned, three different groups of serpentinized peridotites have been defined from the mantle section of the Wizer ophiolite on the basis of chromite chemistry. Less depleted harzburgites have lower Cr# spinels, which partially overlap the fields of both MORB and forearc peridotites. Most harzburgites are highly depleted with spinel compositions that overlap the field of forearc peridotites. Dunite bodies hosted in the highly depleted harzburgites are ultra-depleted with chromite composition similar to those preserved in boninites. It is important to note that despite different degree of depletion of the Wizer

Table 3 Representative serpentine compositions from the Wizer serpentinites

	Less depleted harzburgites				Highly depleted harzburgites				
SiO_2	45.23	46.60	45.29	45.18	45.25	44.28	45.45	44.58	45.79
TiO_2	0.02	0.01	0.02	0.01	0.02	0.02	0.01	0.02	0.01
Al_2O_3	0.19	0.08	0.52	0.16	0.10	0.36	0.22	0.22	0.08
Cr_2O_3	0.61	0.32	0.29	0.14	0.09	0.47	0.22	0.02	0.24
FeO	2.15	1.47	1.17	0.98	0.98	1.22	0.94	1.06	0.93
MnO	0.00	0.00	0.03	0.05	0.05	0.05	0.03	0.03	0.03
MgO	41.88	39.68	40.94	40.98	41.25	40.59	42.13	40.97	41.95
CaO	0.03	0.02	0.05	0.01	0.02	0.06	0.05	0.04	0.02
ZnO	0.11	0.04	0.04	0.01	0.14	0.14	0.05	0.00	0.02
NiO	0.12	0.00	0.01	0.09	0.06	0.14	0.02	0.14	0.06
Total	90.34	88.22	88.36	87.61	87.96	87.33	89.12	87.08	89.13
	Structural formula based on 28 oxygen								
Si	8.119	8.464	8.235	8.276	8.263	8.177	8.196	8.227	8.249
Ti	0.003	0.001	0.003	0.001	0.003	0.003	0.001	0.003	0.001
Al	0.040	0.017	0.111	0.035	0.022	0.078	0.047	0.048	0.017
Cr	0.087	0.046	0.042	0.020	0.013	0.069	0.031	0.003	0.034
Fe^{2+}	0.323	0.223	0.178	0.150	0.150	0.188	0.142	0.164	0.140
Mn	0.000	0.000	0.005	0.008	0.008	0.008	0.005	0.005	0.005
Mg	11.205	10.742	11.095	11.188	11.227	11.172	11.323	11.268	11.263
Zn	0.006	0.004	0.010	0.002	0.004	0.012	0.010	0.008	0.004
Ni	0.015	0.005	0.005	0.001	0.019	0.019	0.007	0.000	0.003
	Highly depleted harzburgites				Dunite bodies				
SiO_2	45.26	44.93	43.35	44.92	44.11	45.03	47.20	45.32	45.15
TiO_2	0.05	0.01	0.07	0.01	0.07	0.00	0.01	0.04	0.00
Al_2O_3	0.29	0.07	0.55	0.10	0.26	0.14	0.36	0.07	0.19
Cr_2O_3	0.16	0.45	0.17	0.15	0.03	0.03	0.43	0.16	0.13
FeO	0.95	1.15	3.67	2.35	3.55	0.98	1.72	0.94	1.35
MnO	0.03	0.00	0.04	0.10	0.01	0.07	0.16	0.05	0.04
MgO	40.73	40.98	39.28	40.14	39.68	41.34	37.90	40.42	42.15
CaO	0.05	0.00	0.06	0.00	0.00	0.01	0.00	0.03	0.02
ZnO	0.26	0.00	0.16	0.01	0.05	0.07	0.00	0.00	0.21
NiO	0.19	0.16	0.50	0.01	0.00	0.09	0.19	0.17	0.03
Total	87.97	87.75	87.85	87.79	87.73	87.76	87.97	87.20	89.27
	Structural formula based on 28 oxygen								
Si	8.271	8.239	8.081	8.269	8.183	8.242	8.594	8.334	8.157
Ti	0.007	0.001	0.010	0.001	0.010	0.000	0.001	0.006	0.000
Al	0.062	0.015	0.121	0.022	0.057	0.030	0.077	0.015	0.040
Cr	0.023	0.065	0.025	0.022	0.040	0.004	0.062	0.023	0.019
Fe^{2+}	0.145	0.176	0.572	0.362	0.551	0.150	0.262	0.145	0.204
Mn	0.005	0.000	0.006	0.016	0.002	0.011	0.025	0.008	0.006
Mg	11.094	11.200	10.913	11.013	10.971	11.278	10.286	11.079	11.350
Zn	0.010	0.000	0.012	0.000	0.000	0.002	0.000	0.006	0.004
Ni	0.035	0.000	0.022	0.001	0.007	0.009	0.000	0.000	0.028

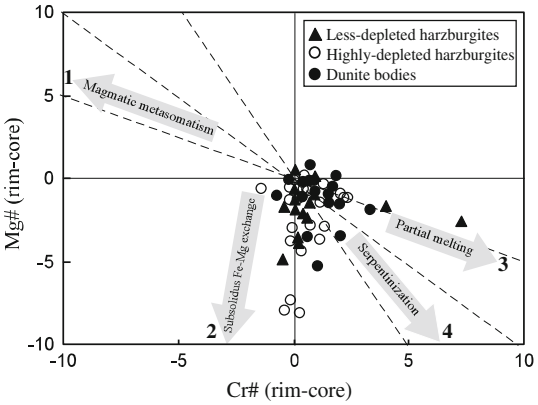

Fig. 8 Diagram showing the rimward compositional variations of the unaltered chromite cores. Each point represents Cr#rim–Cr#core, Mg#rim–Mg#core. The four trends show the rimward enrichment in Al and Mg due to magmatic metasomatism, Cr and Fe related to partial melting, and in Fe slightly and significantly due to subsolidus Fe–Mg exchange with olivine and serpentinization, respectively. These zonation patterns are from Pagé et al. (2008)

peridotites, they have similar and relatively wide ranges of TiO_2 contents. This could reflect interaction with impregnated melts as will be discussed more fully later.

Many authors (e.g. Maurel and Maurel 1982; Kamenetsky et al. 2001; Wasylenki et al. 2003) have shown experimentally that the Al_2O_3 and TiO_2 contents of the parental melts with which the mantle spinel was in equilibrium can be estimated from the spinel compositions. Kamenetsky et al. (2001) inferred, based on spinel-melt inclusion data in volcanic rocks, that there is a linear correlation between Al_2O_3 and TiO_2 contents of spinels and Al_2O_3 and TiO_2 contents, respectively, of their equilibrium melts. Wasylenki et al. (2003) observed similar relation for melt-spinel Al_2O_3 equilibria during peridotite melting. Using this approach, the spinels from the less depleted harzburgites are in equilibrium with melts that have 14.5–15.3 wt% Al_2O_3 and ~<0.38–0.51 wt% TiO_2. The estimated melts composition in equilibrium with spinels from the highly depleted harzburgites have Al_2O_3 of 11.2–14.1 wt% and TiO_2 of <0.09–0.28 wt%. Dunite was in equilibrium with melts containing 9.4–10.6 wt% Al_2O_3 and ~<0.07–0.22 wt% TiO_2. Melts in equilibrium with less depleted harzburgite spinels overlap those of MORB (Al_2O_3 = ~15 wt%; Wilson 1989) and high-Mg island arc tholeiitic (IAT) primary magmas (Al_2O_3 = 11.4–16.4 wt%; Augé 1987). On the other hand, melts in equilibrium with highly depleted harzburgite and dunite spinels overlap those of the high-Mg tholeiites and boninites (Al_2O_3 = 10.6–14.4 wt%; Wilson 1989).

Studies of the overlying crustal section show that these lavas have compositions that formed in equilibrium with the mantle section of the Wizer ophiolite, implying a genetic relationship. Khudeir and Asran (1992) showed that the volcanic sequence of the Wizer ophiolite display a transitional MORB–island arc geochemical affinity. Data of Farahat (2010) for Wizer ophiolitic lavas are consistent with this conclusion and further identified a few dykes with boninitic signature within the volcanic section of the Wizer ophiolite (Fig. 9a). Such genetic relationship between the mantle lithosphere and the overlying crust has been also observed in the classic Mesozoic ophiolites of Cyprus, Oman and California (e.g. Batanova and Sobolev 2000; Le Mée et al. 2004; Choi et al. 2008; Rollinson 2008).

Comparison with the well-studied Semail ophiolites of Oman, which preserves the largest area of mantle harzburgites on Earth, is shown in the Al_2O_3–TiO_2 diagram (Fig. 9a) adopted from Rollinson (2008). The volcanic section of the Oman ophiolite is classified into a basal unit of MORB-like geochemical affinity overlain by upper units of arc-like affinity (Pearce et al. 1981). Boninite lavas and dykes are identified in the upper unit (Ishikawa et al. 2002). These volcanic rocks are genetically related to the low Cr# chromitites, of MORB affinity (Cr# = 52–64) found in the upper part of the mantle section and the high-Cr# chromitites of island arc affinity (Cr# = 71–77) from the lower part of the same mantle section (Rollinson 2005, 2008). The data from the volcanic and mantle sections of the Wizer ophiolite are similar to those from the Oman ophiolite (Fig. 9a). Whole-rock compositions of the Wizer volcanic section, in broad similarity to volcanic section of the Oman ophiolite, occupy both MORB and Oman arc-like fields. On the other hand, the estimated composition of melts in equilibrium with the less depleted harzburgites, including Oman arc-like volcanics, lies between the main MORB array and the depleted mantle melts. Godard et al. (2006) and Rollinson (2008) suggested a mixing model, in which high degree of partial melting (>20%) of a MORB source with a contribution from the melt of more depleted mantle could account for the geochemical and mineralogical features of the Oman upper arc-like lava units and low Cr# chromitites of the shallow mantle. This is similar to situation case of the Wizer less depleted harzburgites, as will be discussed more fully later.

The estimated melts in equilibrium with Wizer highly depleted harzburgites and dunites plot in the depleted mantle field near the boundary of both Oman arc-like volcanics and boninite fields, implying formation via partial melting (or re-melting) of the highly depleted mantle source from which the equilibrium melts of less depleted harzburgites were previously extracted. Plotting the estimated equilibrium melt of dunite bodies within and outside the extremely depleted end of the depleted mantle field supports their ultra-residual nature.

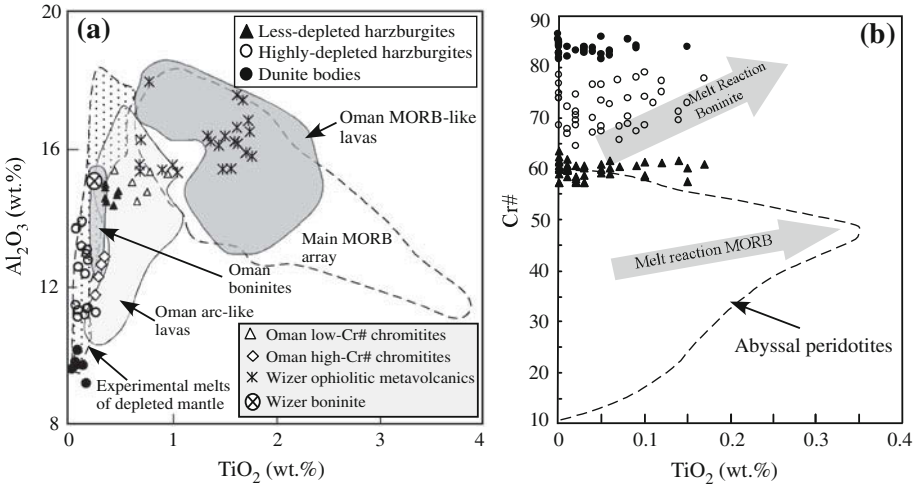

Fig. 9 **a** The estimated compositions of the parental melts to chromites of the Wizer serpentinites and Oman mantle chromitites plotted in TiO_2 versus Al_2O_3 diagram (adopted from Rollinson 2008; after Godard et al. 2006; Ishikawa et al. 2002; Wasylenki et al. 2003) showing comparison with the Wizer and Oman ophiolite volcanic sections. Also, shown are the fields of the main MORB array and melts of depleted mantle (*DM*). Data of the Wizer volcanic section are from Khudeir and Asran (1992) and Farahat (2010). See text for explanation. **b** TiO_2 versus Cr# in chromites of Wizer serpentinites. The abyssel peridotites field and trends of MORB and boninite melt reactions with refractory abyssal peridotites spinel and refractory suprasubduction zone peridotite spinels, respectively, are from Choi et al. (2008)

Petrogenetic evolution

The variability in Cr#, Mg# and TiO_2 contents recorded in the Wizer spinel cores is believed to reflect the compositional evolution of chromite crystallization. The interpretations presented earlier imply that at least three different melts were in equilibrium with the Wizer mantle section. One end-member is a melt of MORB mantle, and the others are both highly depleted and boninitic melts. This signifies that the Wizer mantle section shares a magmatic history that is recognized in the overlying crustal section, which displays transitional MORB–island arc–boninitic geochemical signatures (Fig. 9a).

Partial melting depletes the mantle in its basaltic component. Experimentally, fertile lherzolite source transforms to a residual harzburgite at about 20% melting and dunite at about 50–60% melting (Jaques and Green 1980; Bonatti and Michael 1989; Kostopoulos 1991). Under anhydrous melting conditions, clinopyroxene disappears after ~23% melting in the residual assemblage of peridotite (Falloon et al. 1988; Kinzler and Grove 1993; Wasylenki et al. 2003). The disappearance of clinopyroxene from the source commonly diminishes or stops partial melting especially in the case of fractional melting (Kostopoulos 1991). However, the presence of water, as in the mantle wedge above a subduction zone, has a significant effect on the melting regime since it decreases the relative contributions of olivine and clinopyroxene to the melt, allowing clinopyroxene to persist in the residue phases to higher degree of partial melting (up to 30%) and increases the contribution of orthopyroxene (Gaetani and Grove 1998; Bizimis et al. 2000). An increased contribution of orthopyroxene to the melt would form dunite residue and melts richer in silica such as boninitic or high-Mg andesite melts, which is characteristic of convergent margins (Green and Ringwood 1968; Kushiro 1974). Consequently, the presence of dunite bodies within the Wizer highly depleted harzburgites and the inferred boninitic affinity of their chromites agrees with the suprasubduction origin suggested for the Egyptian ophiolites. Also, the strongly refractory Wizer mantle section can only be formed by hydrous melting in the mantle wedge above a subduction zone.

The mantle section of the Wizer ophiolite shows many petrologic and mineralogical signatures of partial melting. The variations from less depleted to highly depleted harzburgites containing ultra-depleted dunite bodies are associated with systematic changes in chromite compositions (Fig. 6) that are broadly consistent with partial melting origin. This is also consistent with inferences from whole-rock data that these rocks are residues and produced during high degree of melting. Based on experimentally determined residual spinel composition (i.e. equilibrium melting; Hirose and Kawamoto 1995), the Wizer spinel Cr# indicate loss of >45%, 36–43% and 33–35% melt (Fig. 6a) to form dunite, highly depleted harzburgite and less depleted harzburgite, respectively, if the source had a fertile MORB-type mantle composition. These degrees of melting are implausibly high, implying, alternatively, lower degrees of melting of less fertile source (e.g. Seyler et al. 2007). However, the quantitative melting calibration

of Hellebrand et al. (2001) yields lower, more reasonable degrees of melting for dunite bodies (23–22%), highly depleted harzburgites (22–20%) and less depleted harzburgites (19–18%).

Although, as mentioned above, the high apparent melt fraction observed in the strongly refractory Wizer harzburgite–dunite can only be achieved by hydrous melting in the mantle wedge above a subduction zone, some textural and mineralogical data obtained from this study yields some inconsistencies with partial melting as the sole mechanism. The Wizer serpentinized peridotites contain chromites forming euhedral to subhedral grains (Fig. 3c, d), and development of subhedral to anhedral grains with lobate boundaries (Fig. 3e), as would be expected from rocks that have suffered high degree of partial melting, is rarely recorded (Karipi et al. 2007). Furthermore, melt extraction results in spinel that is depleted in TiO_2, such that this oxide decreases with increasing Cr#, which is not seen for the investigated peridotites. Figure 9b shows that some of the Wizer chromites from the highly depleted harzburgites and dunites are enriched in TiO_2, suggesting interaction with an impregnating melt. When depleted peridotite reacts with ultra-depleted melts (e.g. high-Mg andesitic and boninitic), spinel TiO_2 and Cr# both increase, which is observed for highly depleted Wizer harzburgites (Fig. 9b). In contrast, interaction of less depleted peridotite with MORB melts results in spinel that is enriched in TiO_2 without increased Cr# (Choi et al. 2008), which is observed for the Wizer less depleted harzburgites.

In the extremely depleted dunite bodies, the lack of correlation between spinel Cr# and both Mg# and TiO_2 enrichments (Figs. 5, 8b) indicates ultra-residual origin and suggests that a melt–peridotite interaction played a significant role in their genesis. The melt is considered to have been of boninitic composition as it is suggested by the plot of the dunitic chromites in the boninite field in various diagrams and also consistent with the identification of dyke rocks having high-Ca boninitic compositions (Farahat 2010) from the overlying volcanic section. Interestingly, chromite compositions from boninitic volcanic rocks (Cr# = 83–84) are remarkably comparable to those from dunites, signifying petrogenetic linkage. According to Falloon and Danyushevsky (2000), high-Ca boninites represent very high temperature melts (1,400–1,500°C) fluxed with 1–2% H_2O formed at 45 km depth. Rollinson (2008) indicated, based on the model suggested by Falloon and Danyushevsky (2000) for the origin of high-Ca boninite melts, that these melts are expected to cool rapidly on their ascent through the mantle and leave a residue deeper in the mantle compared to the MORB melts. This could accounts to the concentration of the dunite bodies deep in the Wizer mantle section and the rare recognition of boninitic lavas within the overlying volcanic sequence.

Sulfides are important petrogenetic indicators of partial melting and melt–rock interaction, because they concentrate chalcophile trace elements (S, Cu) that partition very similar to CaO and Al_2O_3 (Lorand 1991; Luguet et al. 2003). The identification of sulfides, although rare, within the Wizer harzburgites indicate that they are residual after a maximum of 16% melt extraction from a MORB source (Saal et al. 2002; Luguet et al. 2003), or they were generated by interaction of a highly refractory mantle with a percolative melt (Seyler et al. 2007). The high refractory nature of the investigated mantle section, together with the Cr#-TiO_2 variations discussed above, supports the second interpretation. The identified sulfides resulting from mixing could account to, and can be used as an exploration guide for, the potentially economic deposits of gold associated with the carbonatized ophiolitic peridotites.

To summarize, the correlation between texture and mineral chemistry of chromites from the Wizer ophiolite mantle reveals a multi-stage genesis in the different types of their host peridotites. The combination of partial melting and re-equilibration with percolating melt left a variably depleted peridotite residue. A two-stage partial melting/melt–rock interaction history is proposed. According to this model, a depleted mantle source has interacted with melts of a MORB source mantle to produce the less depleted harzburgites. Later in the history of the ophiolite evolution, a second stage melting of middle refractory (previously melted) harzburgites by interaction with hot melts of high-Mg tholeiites or boninitic compositions formed the highly depleted harzburgites and their host dunite bodies deeper in the mantle. Such a two-stages petrogenetic model has been suggested for other ophiolite sequences (e.g. the Oman and Costal Range of California), which display mineralogical and geochemical features of their mantle and volcanic sections broadly analogous to those of the Wizer ophiolite (e.g. Le Mée et al. 2004; Rollinson 2008; Choi et al. 2008).

Geotectonic implications

It has been shown earlier that spinels in the less depleted harzburgites with lower Cr# resemble those of the more MORB-like peridotites, while those in the highly depleted harzburgites and dunites are analogous to spinels from forearc peridotites. Moreover, the inferred boninitic melt extracted after extensive partial melting of depleted harzburgite to form dunites can only be generated in the mantle wedge above a subduction zone. Some authors suggested that the coexistence of lava and mantle section of MORB and island arc signatures in the same ophiolite sequence

indicates a marginal basin/back arc basin setting for the formation of these ophiolites (e.g. Zhou and Robinson 1997; Godard et al. 2006; Karipi et al. 2007). However, a general consensus exists that the MORB to IAT/boninitic evolution of ophiolites argues for formation in a protoarc-forearc environment (e.g. Arai et al. 2006; Dilek et al. 2007, 2008), pointing to a similar origin for the Wizer ophiolite.

Together with the transition from MORB to IAT/boninitic signature within the Wizer ophiolite sequence, Farahat (2001, 2010) and Farahat et al. (2010) reported a similar systematic lateral change from more MORB-like (in the south) to more IAT–boninite-like (in the north) geochemical affinities of many ophiolitic metavolcanic sequences occurring in the CED. Moreover, the chemistry of chromites from the mantle sequences of the Wadi Ghadir and Wadi El Zarka ophiolites in the extreme southern part of the CED (Fig. 1) is more MORB-like (Cr# = 50–63 and 46–56, respectively; Ahmed et al. 2001) compared to those from ophiolites in the investigated area and in the northern part of the CED generally. This most likely indicates that this part of the Eastern Desert could represent a complete forearc-arc-backarc system above a southeast-dipping (in the present coordinate system) subduction zone. This is further supported by the absence of crustal break in the CED and the separation of CED from the SED by a major shear zone (Fig. 1).

Conclusions

The mantle lithosphere of the Wizer ophiolite sequence provides significant constraints concerning relation to the overlying volcanic section and the petrogenetic and geotectonic evolution of the juvenile Neoproterozoic ANS crust in the Eastern Desert of Egypt. The mineralogical features indicate serpentinization in the mantle wedge beneath a protoarc-forearc, which largely escaped later regional metamorphism. Spinel compositions in serpentinites show a transition from MORB to IAT/boninitic affinity, which is analogous to what is observed in the overlying volcanic sequence, implying a close genetic link. This conclusion is in agreement with conclusions from the classic Mesozoic ophiolites (e.g. Oman, California and Troodos). Melting of depleted harzburgite by reaction with melt of MORB composition followed by second stage melting due to interaction with IAT–bonintic melts best explain the field, geochemical and mineralogical features of the investigated mantle section. The shift from MORB to island arc–boninitic affinities within the mantle lithosphere of the Wizer ophiolite and laterally (from south to north) for ophiolites occurring in the CED implies that this part of the Eastern Desert could represent an arc-backarc system above a southeast-dipping subduction zone. Finally, sulfide minerals, which may have resulted from mixing, along with the presence of carbonate veinlets in the dunite bodies within the mantle section, could be used as an exploration guide for the potentially economic gold deposits, which appear to be related to the carbonatized ophiolitic peridotites.

Acknowledgments The major part of this work has been carried out at the Institute of Earth Sciences, University of Graz during a post-doctor stay of the first author funded by Mission Department, the Egyptian Ministry of Higher Education and Scientific Research. E.S.F. would like to express his sincere appreciation to Profs. C. Hauzenburger, K. Ettinger and F. Walter for their support during XRF, microprobe and XRD analyses, respectively. We thank M. Azer and an anonymous reviewer for their helpful reviews. Manuscript was greatly improved by constructive comments of the Journal editor in topic (R.J. Stern).

References

Abdel Rahman AM, Doig R (1987) The Rb–Sr geochronological evolution of the Ras Gharib segment of the northern Nubian Shield. J Geol Soc Lond 144:577–586

Abu El Ela AM (1996) Contribution to the mineralogy and chemistry of some serpentinites from the Eastern Desert of Egypt. M.E.R.C. Ain Shams Univ Earth Sci Egypt 10:1–25

Ahmed AA (2005) The status of uncertain "ophiolites" in the Eastern Desert of Egypt. In: Proceedings of the 1st symposium classification of the basement complex of Egypt, Assiut Univ., Assiut, Egypt, 16–17 Feb, pp 52–61

Ahmed AH, Arai S, Attia AK (2001) Petrological characteristics of the Pan African podiform chromitites and associated peridotites of the proterozoic ophiolite complexes, Egypt. Miner Deposita 36:72–84

Akaad MK (1997) On the behavior of serpentinites and its implications. Geol Surv Egypt, Paper 74

Akaad MK, Abu El Ela AM (2002) Geology of the basement rocks in the eastern half of the belt between latitudes 25°30′ and 26°30′ N Central Eastern Desert, Egypt. Geol Surv Egypt, Paper 78

Amstutz G, El Gaby S, Ahmed AA, Habib ME, Khudeir AA (1984) Back-arc ophiolite association, Central Eastern Desert, Egypt. Bull Fac Sci Assuit Univ Egypt 13:95–136

Arai S (1992) Chemistry of chromian spinel in volcanic rocks as a potential guide to magma chemistry. Miner Mag 56:173–184

Arai S, Yurimoto H (1994) Podiform chromitites of the Tari-Misaka ultramafic complex, southwestern Japan as mantle-melt interaction products. Econ Geol 89:1279–1288

Arai S, Kadoshima K, Morishita T (2006) Widespread arc-related melting in the mantle of the northern Oman ophiolite as inferred from detrital chromian spinels. J Geol Soc Lond 163:869–879

Augé T (1987) Chromite deposits in the northern Oman ophiolite: mineralogical constraints. Miner Deposita 22:1–10

Azer MK, Khalil AES (2005) Petrological and mineralogical studies of Pan-African serpentinites at Bir Al-Edeid area, Central Eastern Desert, Egypt. J Afr Earth Sci 43:525–536

Azer MK, Stern RJ (2007) Neoproterozoic (835–720 Ma) serpentinites in the Eastern Desert, Egypt: fragments of forearc mantle. J Geol 115:457–472

Barnes SJ (2000) Chromite in komatiites, II. Modifications during greenschist to mid-amphibolite facies metamorphism. J Petrol 41:387–409

Barnes SJ, Roeder PL (2001) The range of spinel compositions in terrestrial mafic and ultramafic rocks. J Petrol 42:2279–2302
Batanova VG, Sobolev AV (2000) Compositional heterogeneity in subduction-related mantle peridotites, Troodos massif, Cyprus. Geology 28:55–58
Bédard JH, Hébert R (1998) Formation of chromitites by assimilation of crustal pyroxenites and gabbros into peridotitic intrusions: North Arm mountain massif, Bay of Islands ophiolite, Newfoundland, Canada. J Geophy Res 103:5165–5184
Beyth M, Stern RJ, Altherr R, Kröner A (1994) The late precambrian Timna igneous complex, southern Israel: evidence for comagmatic-type sanukitoid monzodiorite and alkali granite magma. Lithos 31:103–124
Bizimis M, Salters VJM, Bonatti E (2000) Trace and REE content of clinopyroxenes from supra-subduction zone peridotites. Implications for melting and enrichment processes in islands arcs. Chem Geol 165:67–85
Bonatti E, Michael PJ (1989) Mantle peridotites from continental rifts to ocean basins to subduction zones. Earth Planet Sci Lett 91:297–311
Caran Ş, Coban H, Flower MFJ, Ottley CJ, Yilmaz K (2010) Podiform chromitites and mantle peridotites of the Anatalya ophiolite, Isparta Angle (SW Turkey): implications for partial melting and melt-rock interaction in oceanic and subduction-related settings. Lithos 114:307–326
Choi SH, Shervais JW, Mukasa SB (2008) Supra-subduction and abyssal mantle peridotites of the coast range ophiolite, California. Contrib Miner Petrol 156:551–576
Dick HJB (1989) Abyssal peridotites, very slow spreading ridges, and ocean ridge magmatism. In: Saunders AJ, Norry MJ (eds) Magmatism in the oceanic basins. Geol Soc Lond Spec Pub 42:71–105
Dick HJB, Bullen T (1984) Chromian spinel as a petrogenetic indicator in abyssal and alpine-type peridotite and spatially associated lavas. Contrib Miner Petrol 86:54–76
Dilek Y, Furnes H, Shallo M (2007) Suprasubduction zone ophiolite formation along the periphery of mesozoic Gondwana. Gondwana Res 11:453–475
Dilek Y, Furnes H, Shallo M (2008) Geochemistry of the Jurassic mirdita ophiolite (Albania) and the MORB to SSZ evolution of a marginal basin oceanic crust. Lithos 100:174–209
Dixon TH, Golombek MP (1988) Late precambrian crustal accretion rates in Northeast Africa and Arabia. Geology 16:991–994
Droop GTR (1987) A general equation for estimating Fe^{3+} concentrations in ferromagnesian silicates and oxides from microprobe analyses, using stoichiometric criteria. Miner Mag 51:431–435
El Bahariya GA, Arai S (2003) Petrology and origin of Pan-African serpentinites with particular reference to chromian spinel compositions, Eastern Desert, Egypt: implication for supra-subduction zone ophiolite. In: Proceedings of 3rd international conference on geology of Africa, Assiut Univ, Egypt, pp 371–388
El Gaby S (2005) Integrated evolution and rock classification of the Pan-African belt in Egypt. In: Proceedings of the 1st symposium classification of the basement complex of Egypt, pp 1–9
El Gaby S, List FK, Tehrani R (1988) Geology, evolution and metallogenesis of the Pan-African belt in Egypt. In: El Gaby S, Greiling RO (eds) The Pan-African belt of NE Africa and adjoining areas. Vieweg, Braunschweig, pp 289–316
El-Sayed MM, Furnes H, Mohamed FH (1999) Geochemical constraints on the tectonomagmatic evolution of the late precambrian Fawakhir ophiolite, Central Eastern Desert, Egypt. J Afr Earth Sci 29:515–533
El Sharkawy MA, El Bayoumi RM (1979) The ophiolites of Wadi Ghadir area Eastern Desert, Egypt. Ann Geol Surv Egypt 9:125–135
Evans BW (1977) Metamorphism of alpine peridotite and serpentinite. Ann Rev Earth Planet Sci 5:397–447
Falloon TJ, Danyushevsky LV (2000) Melting of refractory mantle at 1.5, 2.0 and 2.5 GPa under anhydrous and H2O undersaturated conditions: implications for the petrogenesis of high-Ca boninites and the influence of subduction components on mantle melting. J Petrol 41:257–283
Falloon TJ, Green DH, Hatton CJ, Harris KL (1988) Anhydrous partial melting of a fertile and depleted peridotite from 2 to 30 kb and application to basalt petrogenesis. J Petrol 29:1257–1282
Farahat ES (2001) Comparative petrological studies of some pillowed lavas in the Eastern Desert, Egypt. Unpublished PhD Thesis, Minia Univ., Egypt, p 251
Farahat ES (2006) The Neoproterozoic Kolet Um Kharit bimodal metavolcanic rocks, south Eastern Desert, Egypt: a case of enrichment from plume interaction? Int J Earth Sci 95:275–287
Farahat ES (2008) Chrome-spinels in serpentinites of the El Ideid-El Sodmein district, Central Eastern Desert, Egypt: their metamorphism and petrogenetic implications. Chem Erde 68:193–205
Farahat ES (2010) Neoproterozoic arc-back-arc system in the Central Eastern Desert of Egypt: evidence from supra-subduction zone ophiolites. Lithos. doi:10.1016/j.lithos.2010.08.017
Farahat ES, El Mahallawi MM, Hoinkes G, Abdel Aal AY (2004) Continental back-arc basin origin of some ophiolites from the Eastern Desert of Egypt. Miner Petrol 82:81–104
Farahat ES, El Mahallawi MM, Hoinkes G, Abdel Aal AY, Hauzenberger C (2010) Pillow form morphology of selected neoproterozoic metavolcanics in the Egyptian Central Eastern Desert and their implications. J Afr Earth Sci 57:163–168
Gaetani GA, Grove TL (1998) The influence of water on melting of mantle peridotite. Contrib Miner Petrol 131:323–346
Godard M, Bosch D, Einaudi F (2006) A MORB source for low-Ti magmatism in the Semail ophiolite. Chem Geol 234:58–78
Green TH, Ringwood AE (1968) Genesis of the calc-alkaline igneous rock suite. Contrib Miner Petrol 18:105–162
Hargrove US, Stern RJ, Kimura J-I, Manton WI, Johnson PR (2006) How juvenile is the Arabian–Nubian shield? Evidence from Nd isotopes and pre-neoproterozoic inherited zircon in the Bi'r Umq suture zone, Saudi Arabia. Earth Planet Sci Lett 252:308–326
Hellebrand E, Snow JE, Dick HJB, Hoffmann AW (2001) Coupled major and trace elements as indicators of the extent of melting in mid-ocean-ridge peridotites. Nature 410:677–681
Hellebrand E, Snow JE, Hoppe P, Hofmann AW (2002) Garnet field melting and late stage refertilization in residual abyssal peridotites from the Central Indian ridge. J Petrol 43:2305–2338
Hirose K, Kawamoto T (1995) Hydrous partial melting of lherzolite at 1GPa: the effect of H_2O on the genesis of basaltic magmas. Earth Planet Sci Lett 133:463–473
Hume WF (1935) Geology of Egypt. Geol Surv Egypt 2:2
Hyndman RD, Peacock SM (2003) Serpentinization of the forearc mantle. Earth Planet Sci Lett 212:417–432
Ishii T, Robinson PT, Maekawa H, Fiske R (1992) Petrological studies of peridotites from diapiric serpentinite seamounts in the Izu-Ogasawara-Mariana forearc, leg 125. In: Proceedings on Ocean Drilling Program, Scientific Results 125. College Station, TX, Ocean Drilling Program, pp 445–485
Ishikawa T, Nagaishi K, Umino S (2002) Boninitic volcanism in the Oman ophiolite: implications for thermal condition during transition from spreading ridge to arc. Geology 30:899–902
Jaques AL, Green DH (1980) Anhydrous melting of peridotite at 0–15 kb pressure and the genesis of tholeiitic basalts. Contrib Miner Petrol 73:287–310
Johnson KTM, Dick HJB, Shimizu N (1990) Melting in the oceanic upper mantle; an ion microprobe study of diopsides in abyssal peridotites. J Geophys Res 95:2661–2678

Kamenetsky V, Crawford AJ, Meffre S (2001) Factors controlling chemistry of magmatic spinel: an empirical study of associated olivine, Cr-spinel and melt inclusions from primitive rocks. J Petrol 42:655–671

Karipi S, Tsikouras B, Hatzipanagiotou K, Grammatikopoulos TA (2007) Petrogenetic significance of spinel-group minerals from the ultramafic rocks of the Iti and Kallidromon ophiolites (Central Greece). Lithos 99:136–149

Khalil AES, Azer MK (2007) Supra-subduction affinity in the neoproterozoic serpentinites in the Eastern Desert, Egypt: evidences from mineral composition. J Afr Earth Sci 49:136–152

Khudeir AA (1995) Chromian spinel-silicate chemistry in peridotite and orthopyroxenite relicts from ophiolitic serpentinites, Eastern Desert, Egypt. Bull Fac Sci Assuit Univ Egypt 24:221–261

Khudeir AA, Asran HA (1992) Back-arc Wizer ophiolites at Wadi Um Gheig district, Eastern Desert, Egypt. Bull Fac Sci Assiut Univ Egypt 21:1–22

Khudeir AA, El Haddad MA, Leake BE (1992) Compositional variation in chromite from the Eastern Desert. Miner Mag 56:567–574

Kinzler RJ, Grove TL (1993) Corrections and further discussion of the primary magmas of mid-ocean ridge basalts, 1 and 2. J Geophys Res 98:22339–22348

Kostopoulos D (1991) Melting of the shallow upper mantle. J Petrol 32:671–699

Kröner A, Pallister JS, Fleck RJ (1992a) Age of initial oceanic magmatism in the late proterozoic Arabian shield. Geology 20:803–806

Kröner A, Todt W, Hussein IM, Mansour M, Rashwan AA (1992b) Dating of late proterozoic ophiolites in Egypt and the Sudan using the single grain zircon evaporation technique. Precam Res 59:15–32

Kushiro I (1974) Melting of hydrous upper mantle and possible generation of andesite magma. An approach from synthetic systems. Earth Planet Sci Lett 22:294–299

Le Mée L, Girardeau J, Monnier C (2004) Mantle segmentation along the Oman ophiolite fossil mid-ocean ridge. Nature 432:167–172

Lorand JP (1991) Sulfide petrology and sulfur geochemistry of orogenic lherzolites: a comparative study between Pyrenean bodies (France) and the Lanzo massif (Italy). In: Menzies MA et al (eds) Orogenic lherzolites and mantle processes. J Petrol, pp 77–95

Luguet A, Lorand JP, Seyler M (2003) A coupled study of sulfide petrology and highly siderophile element geochemistry in abyssal peridotites from the Kane fracture zone (MARK area, mid-Atlantic ridge). Geochim Cosmochim Acta 67:1553–1570

Maurel C, Maurel P (1982) Étude expérimental de la distribution de l'aluminium entre bain silicate basique et spinelle chromifére. Implications pétrogenetiques: teneur en chrome des spinelles. Bulletin de Mineralogie 105:197–202

Meert JG (2003) A synoposis of events related to the assembly of eastern Gondwana. Tectonophysics 362:1–40

Niu Y (1997) Mantle melting and melt extraction processes beneath ocean ridges: evidence from abyssal peridotites. J Petrol 38:1047–1074

Niu Y (2004) Bulk-rock major and trace element compositions of abyssal peridotites: implications for mantle melting, melt extraction and post-melting processes beneath mid-ocean ridges. J Petrol 45:2423–2458

Noweir AM, Ghoneim MF, El-Anwar MA (1983) Geology and lithostratigraphy of the Pre-cambrian around Um Gheig, Eastern Desert, Egypt. In: Proceedings of the 5th International Conference on Basement Tectonics, pp 77–83

Pagé P, Bédard JH, Schroetter JM, Tremblay A (2008) Mantle petrology and mineralogy of the Thetford mines Ophiolite complex. Lithos 100:255–292

Palandri JL, Reed MH (2004) Geochemical models of metasomatism in ultramafic systems: serpentinization, rodingitization and sea floor carbonate chimney precipitation. Geochim Cosmochim Acta 68:1115–1133

Patchett PJ, Chase CG (2002) Role of transform continental margins in major crustal growth episodes. Geology 30:39–42

Paulick H, Bach W, Godard M, De Hoog JCM, Suhr G, Harvey J (2006) Geochemistry of abyssal peridotites (mid-Atlantic ridge, 15°20′N, ODP Leg 209): implications for fluid/rock interaction in slow spreading environments. Chem Geol 234:179–210

Pearce JA, Alabaster T, Shelton AW, Searle MP (1981) The Oman ophiolite as a cretaceous arc-basin complex: evidence and implications. Philos Trans R Soc Lond A300:299–317

Rittmann A (1958) Geosynclinal volcanism, ophiolites, and barramiya rocks. Egypt J Geol 2:61–66

Rollinson H (2005) Chromite in the mantle of the Oman ophiolite: a new genetic model. Island Arc 14:542–550

Rollinson H (2008) The geochemistry of mantle chromitites from the northern part of the Oman ophiolite: inferred parental melt compositions. Contrib Miner Petrol 156:273–288

Saal AE, Hauri EH, Langmuir CH, Perfit MR (2002) Vapour undersaturation in primitive mid-ocean-ridge basalt and the volatile content of Earth's upper mantle. Nature 419:451–455

Sabet AH (1961) Geology and mineral deposits of Gabal El-Sibai area, Red Sea hills, Egypt. Ph.D. thesis, Leiden State University, The Netherland

Seyler M, Lorand JP, Dick HJB, Drouin M (2007) Pervasive melt percolation reactions in ultra-depleted refractory harzburgites at the mid-Atlantic ridge, 15–20 N: ODP Hole 1274A. Contrib Miner Petrol 153:303–319

Shackleton RM (1994) Review of late Proterozoic sutures, ophiolitic mélanges and tectonics of eastern Egypt and north Sudan. Geologische Rundschau 83:537–546

Stein M, Hofmann AW (1994) Mantle plumes and episodic crustal growth. Nature 372:63–68

Stern RJ (1994) Arc assembly and continental collision in the neoproterozoic east African orogen: implications for the consolidation of Gondwana. Ann Rev Earth Planet Sci Lett 152:75–91

Stern RJ, Gwinn CJ (1990) Origin of late precambrian intrusive carbonates, Eastern Desert of Egypt and Sudan: C, O and Sr isotopic evidences. Precam Res 46:259–272

Stern RJ, Hedge C (1985) Geochronologic and isotopic constraints on late Precambrian crustal evolution in the Eastern Desert of Egypt. Am J Sci 285:97–127

Stern RJ, Johnson PR, Kröner A, Yibas B (2004) Neoproterozoic ophiolites of the Arabian-Nubian shield. In: Kusky TM (ed) Precambrian ophiolites and related rocks. Dev Precamb Geol 13:95–128

Takla MA, Noweir AM (1980) Mineralogy and mineral chemistry of the ultramafic mass of El Rabshi Eastern Desert, Egypt. Neues Jahrb Mineral Abh 140:17–28

Ulmer P, Trommsdorf V (1995) Serpentine stability to mantle depths and subduction-related magmatism. Science 268:858–861

Wasylenki LE, Baker MB, Kent AJR, Stolper EM (2003) Near solidus melting of the shallow upper mantle: partial melting experiments on depleted peridotite. J Petrol 4:1163–1191

Wilson M (1989) Igneous petrogenesis. A global tectonic approach. Chapman and Hall, London, p 466

Zhou M-F, Robinson PT (1997) Origin and tectonic environment of podiform chromite deposits. Econ Geol 92:259–262